Published in final edited form as:
Urol Res. 2010 December ; 38(6): 491–495. doi:10.1007/s00240-010-0319-9.

Novel ultrasound method to reposition kidney stones

Anup Shah,
University of Washington, School of Medicine, Department of Urology, 1959 NE Pacific St, Seattle, WA 98195, anupshah@u.washington.edu

Neil R. Owen,
University of Washington, Applied Physics Laboratory, Center for Industrial and Medical Ultrasound, 1013 NE 40th St, Seattle, WA 98105

Wei Lu,
University of Washington, Applied Physics Laboratory, Center for Industrial and Medical Ultrasound, 1013 NE 40th St, Seattle, WA 98105

Bryan W. Cunitz,
University of Washington, Applied Physics Laboratory, Center for Industrial and Medical Ultrasound, 1013 NE 40th St, Seattle, WA 98105

Peter J. Kaczkowski,
University of Washington, Applied Physics Laboratory, Center for Industrial and Medical Ultrasound, 1013 NE 40th St, Seattle, WA 98105

Jonathan D. Harper,
University of Washington, School of Medicine, Department of Urology, 1959 NE Pacific St, Seattle, WA 98195

Michael R. Bailey, and
University of Washington, Applied Physics Laboratory, Center for Industrial and Medical Ultrasound, 1013 NE 40th St, Seattle, WA 98105 bailey@apl.washington.edu

Lawrence A. Crum
University of Washington, Applied Physics Laboratory, Center for Industrial and Medical Ultrasound, 1013 NE 40th St, Seattle, WA 98105

Abstract

The success of surgical management of lower pole stones is principally dependent on stone fragmentation and residual stone clearance. Choice of surgical method depends on stone size, yet all methods are subject to post-surgical complications resulting from residual stone fragments. Here we present a novel method and device to reposition kidney stones using ultrasound radiation force delivered by focused ultrasound and guided by ultrasound imaging. The device couples a commercial imaging array with a focused annular array transducer. Feasibility of repositioning stones was investigated by implanting artificial and human stones into a kidney-mimicking phantom that simulated a lower pole and collecting system. During experiment, stones were located by ultrasound imaging and repositioned by delivering short bursts of focused ultrasound. Stone motion was concurrently monitored by fluoroscopy, ultrasound imaging, and video photography, from which displacement and velocity were estimated. Stones were seen to move immediately after delivering focused ultrasound and successfully repositioned from the lower pole to the collecting system. Estimated velocities were on the order of 1 cm/s. This *in vitro* study demonstrates a promising modality to facilitate spontaneous clearance of kidney stones and increased clearance of residual stone fragments after surgical management.

Keywords

lower pole renal calculi; stone free rate; stone position; ultrasound

1 Introduction

Optimal surgical management of lower pole calyx renal calculi remains a controversial topic as well as a treatment dilemma for the practicing urologist. In a prospective randomized clinical trial, the Lower Pole Study Group determined that the stone free rates for lower pole stones were significantly better for patients treated with percutaneous nephrolithotomy (PCNL) compared to extracorporeal shock wave lithotripsy (ESWL) with the largest observed difference seen in stones greater than 1 cm in diameter [1]. With recent technological advancements, ureteroscopic management has shown stone free rates comparable to those of ESWL for stones <1 cm in diameter [2].

Despite the evolution of technology-driven surgical approaches, the success in surgical management of lower pole stones is principally dependent on two processes: stone fragmentation and residual fragment clearance. The clinical need to establish complete stone clearance is highlighted by Chen and Streem [3] who prospectively followed 206 patients with isolated lower pole calculi treated with ESWL. This study concluded that post-ESWL the probabilities of a symptomatic episode or requiring intervention at 5 years were 0.24 and 0.52, respectively.

Pelvic-caliceal anatomic factors including infundibulopelvic angle, infundibular length, and spatial orientation of caliceal anatomy have been identified as factors that may prospectively predict success of ESWL treatment for lower pole stones [4]. These anatomic factors have been proposed to hinder stone clearance and as such, percussion, diureses, and inversion therapy have all been proposed as adjunctive post-ESWL treatments to optimize stone clearance [5, 6, 7].

To date, no research has been performed investigating the use of ultrasound radiation force as a mechanism to improve stone clearance and post-surgical stone free rates. We describe the development and *in vitro* testing of a prototype device that uses non-invasive ultrasound imaging to guide the application of focused ultrasound to move stones within the renal collecting system. The goal of this new device is to guide lower pole fragments out of a dependent caliceal position to a more superior position to facilitate spontaneous clearance of stone fragments.

2 Methods

Acoustic radiation force results from the transfer of acoustic wave momentum to an absorbing object, and is one example of a universal phenomenon associated with all forms of wave motion [8]. In the context of noninvasive repositioning of kidney stones and stone fragments in the lower pole and collecting system, the force acting on the stones is effectively contained, because of the acoustic pressure profile, within the focused beam and principally along the propagation axis. Therefore, with proper alignment of a focused beam upon a stone, it can be guided to a position that promotes spontaneous clearance or, for larger stones, increases the efficacy of stone removal therapies.

Figure 1 shows a schematic drawing of the hand-held probe for ultrasound-guided stone repositioning. It includes two ultrasound probes: a commercial imaging probe (HDI P4-2, Philips Healthcare, Andover, MA) and a focused ultrasound probe. An HDI 5000 (Philips

Healthcare, Andover, MA) generated ultrasound images that were used to visualize and target the stones. The focused probe consists of an 8-element annular array with a nominal frequency of 2.0 MHz. Diameter of the active area was 63 mm and diameter of the inner imaging aperture was 20 mm. Array elements were driven by separate amplifiers and by adjusting phase delays the focal depth was programmable within a range of 4.5 cm to 8.5 cm. Figure 2 shows a numerical simulation of the focused acoustic beam, and is exemplary of the spatial precision with which the stone-repositioning ultrasound can be delivered. Ultrasound was coupled to the tissue phantom by a water-filled stand off.

A kidney phantom was created using an optically-transparent gel [9]. While the gel polymerized, a void to simulate a collecting system and lower pole was created using the cast of a 18F silicone Foley catheter. Artificial stones, metal-plated glass beads from 2.5 mm to 4.0 mm in diameter, and human urinary calculi, from 3 mm to 8 mm in diameter, were placed dependently in the simulated collecting system. Figure 3 shows a photograph of an artificial stone within the kidney phantom. Human urinary calculi consisted of calcium oxalate and calcium hydrogen phosphate dihydrate (also known as brushite) and were >90% in purity. These stones were rehydrated for more than 24 hours before experiment.

Once placed in the simulated lower pole, stones were located and visualized by ultrasound imaging. Coaxial arrangement of the imaging and focused probes permitted positioning of the device to locate the stone within the imaging plane and within the programmed focal volume of the annular array. Focused ultrasound was then delivered at instantaneous acoustic power of 5 W to 40 W, duty cycle of 50%, and duration of 2 s to 5 s. Stone motion in the kidney phantom was concurrently monitored by fluoroscopy and video photography, from which velocity, displacement, and trajectory were recorded.

3 Results

In the kidney phantom, delivery of focused ultrasound resulted in stone motion from the lower pole into the collecting system. Stone motion was seen immediately after application of the focused ultrasound and stone velocity was on the order of 1 cm/s. Figure 4 shows fluoroscopic images of an artificial stone's initial position in the lower pole, trajectory in response to focused ultrasound, and final position within the collecting system. Stone motion and repositioning were observed for both artificial and human urinary stones and were independent of stone size. Operators could generally control the direction of stone displacement and we found that the best angle of focused ultrasound exposure was in line with the simulated infundibulum. However, this angle could be difficult to determine extracorporeally.

All powers used moved the stones with essentially the same rate, but at least 10 W was required to lift the largest stone, 8 mm, all the way to the collecting system. As many as 6 stones placed in the collecting system at one time were all repositioned to the lower pole. Although energy was directed toward the collection of small stones and could lift slightly many stones at once, only one stone was repositioned to the collecting system with each pulse. Additionally, stone motion was not observed at all angles of focused ultrasound delivery. Angles of focus that were parallel to the axis of the simulated infundibulum resulted in larger displacement.

Figure 5 shows ultrasound images analogous to the fluoroscopy images in Fig. 4, and demonstrates how the integration of imaging focused ultrasound can be used to detect and target residual stones, reposition them in the collecting system, and provide the user with real time visual feedback. Hyper-echogenic vertical bands on the edges of Fig. 5B resulted from delivery of focused ultrasound and illustrate how ultrasound imaging can be

synchronized to maintain visualization of the stone. Figure 6 shows video photography monitoring analogous to fluoroscopy and ultrasound.

Although this was an *in vitro* study to evaluate feasibility, the low potential of *in vivo* tissue injury can be assessed by comparing acoustic intensities to the limits determined by the FDA for diagnostic ultrasound imaging: $I_{SPPA} \leq 190$ W/cm^2 to prevent cavitational injury and $I_{SPTA} \leq 720$ mW/cm^2 to prevent thermal injury [10]. Focal intensities can be estimated as total acoustic power delivered by the transducer per cross sectional area of the focal beam width. A total power of 10 W, enough to lift the largest stone in this study, relates to focal intensity of 10 W/π0.3^2, or approximately 30 W/cm^2. This is the spatial-averaged pulse-average intensity, I_{SAPA}, that must be multiplied by 1.6 [11] to attain the spatial-peak pulse-averaged intensity, I_{SPPA}, 45 W/cm^2, which is lower than the FDA limit. The spatial-peak time-averaged intensity, I_{SPTA}, is I_{SPPA} multiplied by the temporal duty factor, 50%, or 23 W/cm^2, which is higher than the FDA limit. However, because exposure times to reposition stones were 2 s to 5 s, as opposed to tens of minutes for diagnostic ultrasound, the risk of thermal injury is low. As another point of comparison, intensities 2 to 3 orders of magnitude higher, I_{SPTA} of 1500 - 15,000 W/cm^2, such as those used for high intensity focused ultrasound (HIFU), are necessary to induce tissue necrosis during similar exposure times [12].

4 Discussion

The goal of elective renal stone surgery is to render the patient stone free. Persistent renal fragments remaining after stone comminution is common after the treatment of lower pole stones due to their dependent position and pelvic-caliceal anatomic factors. We have described a novel ultrasound-guided therapy to aid in stone fragment expulsion.

As expected, larger stones were the most difficult to reposition and perhaps this observation is due to higher stone mass as well as difficult maneuvering past a narrow infundibular channel. This technology is not dependent on stone composition as a variety of common human calculi subtypes were able to be repositioned.

Advantages of this new technology include hand-held portability, reusability, and no required sterilization. As ultrasound exposure has no known harmful side-effects and is a painless exposure, the device could be potentially used in awake, non-anesthetized patients in a clinic or emergency room setting.

Potential applications for this device also include adjunctive use with primary medical expulsive therapy and the management of obstructing ureteropelvic junction stones by pushing the stone back into a non-obstructing location. The device may also be used in patients with known infectious stones where it has been well established that complete stone clearance is essential to prevent further stone formation as well as reduce the likelihood of recurrent infection. Lastly, this ultrasound-based device may also be used in the management of renal calculi in the pediatric and pregnant populations where there is greater concern over effects of ionizing radiation [13] common to ureteroscopic, SWL, and percutaneous stone management.

Acknowledgments

We thank our colleagues at the Center for Industrial and Medical Ultrasound and the Consortium for Shock Waves in Medicine for advice, shared resources, and review.

This work was supported by a grant from the National Space Biomedical Research Institute NCC9-58, NIH DK43881, and NIH DK086371.

References

1. Albala DM, Assimos DG, Clayman RV. Lower pole I: A prospective randomized trial of extracorporeal shock wave lithotripsy and nephrostolithotomy for lower pole nephrolitiasis - Initial results. Journal of Urology. 2001; 166(2072)
2. Pearle MS, Lingeman JE, Leveilee R. Prospective randomized trial comparing shock wave lithotripsy and ureteroscopy for lower pole caliceal calculi 1 cm or less. Journal of Urology. 2008; 179(S69)
3. Chen RN, Streem SB. Extracorporeal shock wave lithotripsy for lower pole calculi: Long-term radiographic and clinial outcome. Journal of Urology. 1996; 156(1572)
4. Sampaio FJ, Aragao AH. Limitations of extracorporeal shockwave lithotripsy for lower caliceal stones: Anatomic insight. J Endourology. 1994; 8(241)
5. Chiong E, Hwee ST, Kay LM. Randomized controlled study of mechanical percussion, diuresis, and inversion therapy to assist passage of lower pole renal calculi after shock wave lithotripsy. Journal of Urology. 2005; 65(1070)
6. Kekre NS, Kumar S. Optimizing the fragmentation and clearance after shock wave lithotripsy. Curr Opin Urol. 2008; 18(205)
7. Pace KT, Tariq N, Dyer SJ. Mechanical percussion, inversion, and diuresis for residual lower pole fragments after shock wave lithotripsy: A prospective, single blind, randomized controlled trial. Journal of Urology. 2001; 166(2065)
8. Torr GR. The acoustic radiation force. Journal of the Acoustical Society of America. 1984; 52(5): 402–408.
9. Lafon C, Zderic V, Noble ML, Yuen JC, Kaczkowski PJ, Sapozhnikov OA, Chavrier F, Crum LA, Vaezy S. Gel phantom for use in high intensity focused ultrasound dosimetry. Ultrasound in Medicine and Biology. 2005; 31(10):1383–1389. [PubMed: 16223642]
10. Information for Manufacturers Seeking Marketing Clearance for Diagnostic Ultrasound Systems and Transducers. U.S. Food and Drug Administration; 2008.
11. O'Neil HT. Theory of focusing radiators. Journal of the Acoustical Society of America. 1949; 21(5):516–526.
12. Bailey MR, khokhlova VA, Sapozhnikov OA, Kargl SG, Crum LA. Physical mechanisms of the therapeutic effect of ultrasound (a review). Acoustical Physics. 2003; 49(4):369–388.
13. Smith-Bindman R, Lipson J, Marcus R, Kim KP, Mahesh M, Gould R, de Gonzalez AB, Miglioretti DL. Radiation dose associated with common computed tomography examinations and the associated lifetime attributable risk of cancer. Arch Intern Med. 2009; 169(22):2078–2086. [PubMed: 20008690]

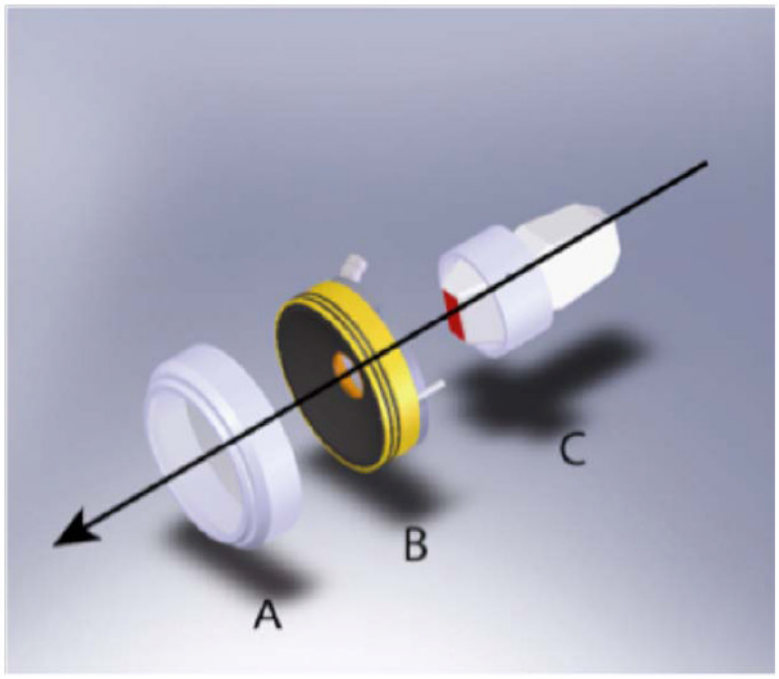

Fig. 1.
Schematic diagram of the hand-held probe for ultrasoundguided repositioning of kidney stones: (A) the coupling standoff, (B) the focused annular array transducer, and (C) the ultrasound scan head. Coaxial arrangement of the probes places the focused ultrasound beam within the image plane.

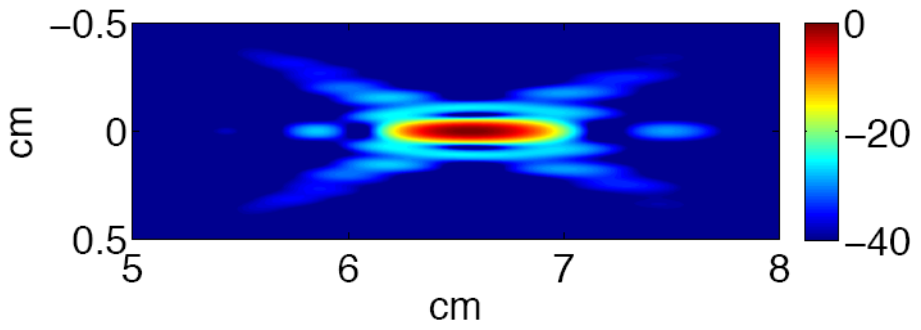

Fig. 2.

Simulation of the focused ultrasound beam, from the annular array propagating from left to right, at a programmed focal depth of 6.5 cm. The beam width was 0.6 cm and 1.1 cm at -6 dB and -20 dB, respectively. Scale in dB.

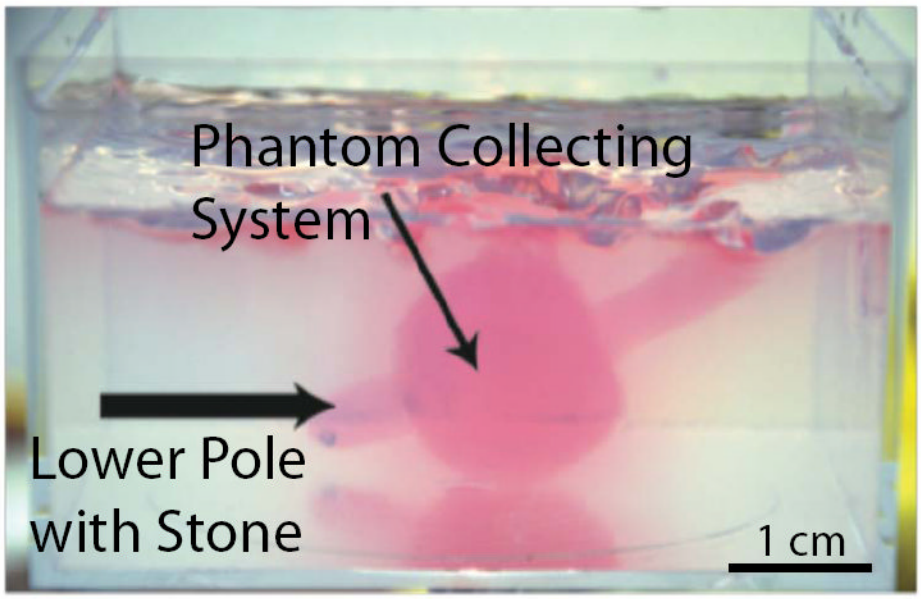

Fig. 3.

Photograph of the kidney phantom with a simulated collecting system and lower pole. Artificial and human stones were placed dependently in the lower pole, and were repositioned to the collecting system using the ultrasound-guided therapy device. The hand-held source was in contact with the lower side of the phantom with its axis aimed vertically through the phantom. Stone repositioning in the transparent phantom was monitored concurrently with fluoroscopy, ultrasound imaging, and video photography.

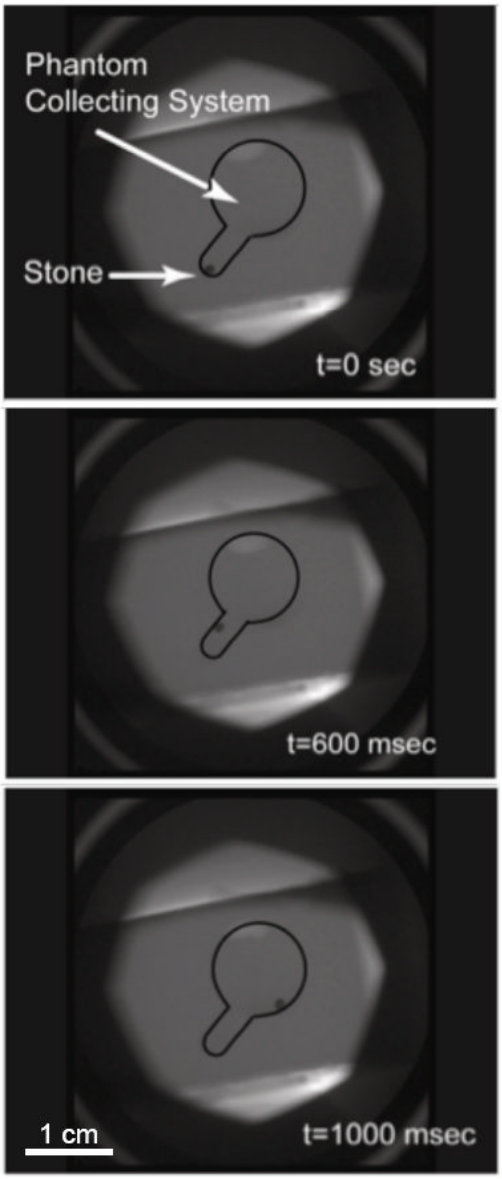

Fig. 4.

Fluoroscopy monitoring of an artificial stone that was repositioned from the lower pole into the collection system of a kidney phantom. Displacement of the stone was seen immediately after the application of focused ultrasound and the total distance traveled was approximately 1 cm. Estimated velocity magnitude was 1 cm/s.

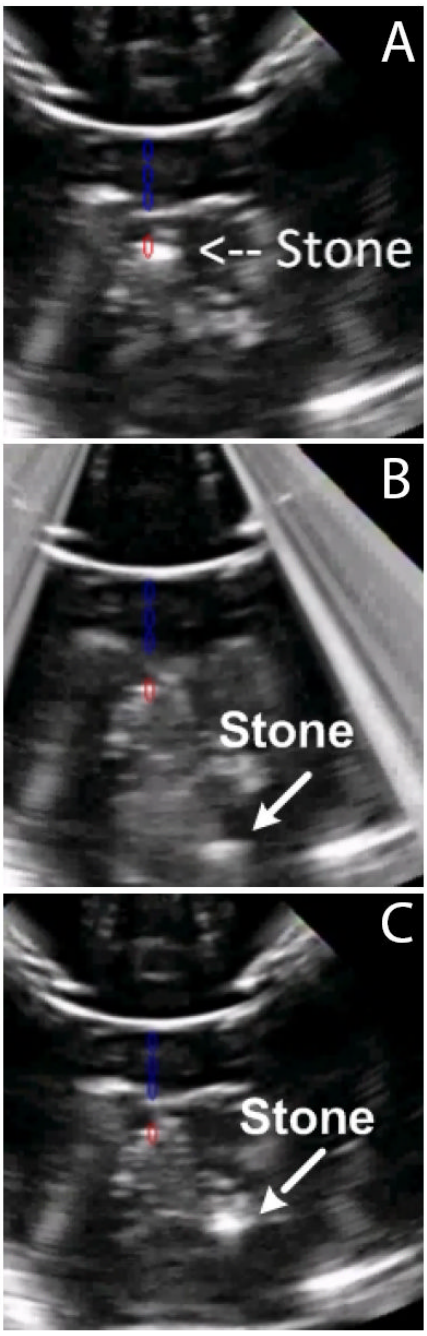

Fig. 5.

Ultrasound monitoring of an artificial stone (a) before, (b) during, and (c) after delivering focused ultrasound to move the stone from the lower pole to the collecting system of the kidney phantom. Blue artifacts were added to denote the axis of the focused array, and the red artifact shows its focus; (a) shows initial targeting of the stone. The lower pole appears at the top of these images because the hand-held device was in contact with the bottom of the phantom.

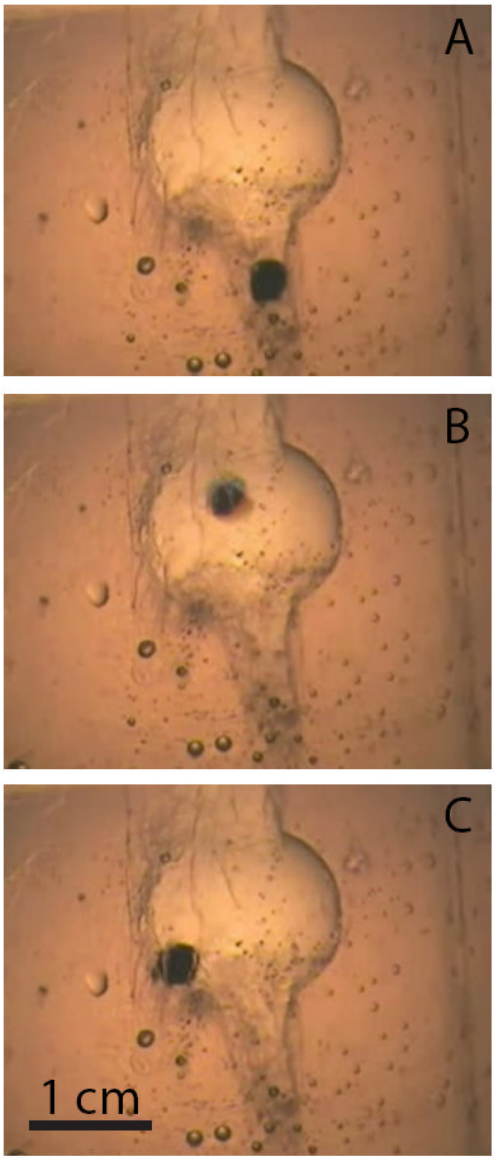

Fig. 6.
Video photography monitoring of an artificial stone (a) before, (b) during, and (c) after delivering focused ultrasound.